# Increased rates of tRNA charging through modification of the enzyme–aminoacyl-adenylate complex of phenylalanyl-tRNA synthetase

Michael Ibba[a,*], Christopher M. Johnson[b], Hauke Hennecke[a], Alan R. Fersht[b]

[a]*Mikrobiologisches Institut, Eidgenössische Technische Hochschule, ETH Zentrum, Schmelzbergstrasse 7, CH-8092 Zürich, Switzerland*
[b]*Cambridge Centre for Protein Engineering, MRC Centre, Hills Road, Cambridge CB2 2QH, UK*

Received 22 December 1994

**Abstract The transfer of amino acid to tRNA by *Escherichia coli* phenylalanyl-tRNA synthetase (PheRS) was studied using replacements of Ala[294] in the $\alpha$ subunit previously shown to have modified amino acid specificity. Steady-state analysis of tRNA charging showed little difference between wild-type and mutants, whereas pre-steady-state analysis revealed higher rates of tRNA charging by both the A294S PheRS-phenylalanyl adenylate and the A294G PheRS-*p*-Cl-phenylalanyl adenylate. The decrease in energy required for the formation of the transition state of amino acid transfer in these mutants could be related to a weaker binding of the amino acid in the aminoacyl adenylate complex. Thus a compromise appears to exist between amino acid activation and tRNA charging, because slowing down the first step increases the rate of the second step, possibly as a result of decreased stability of the PheRS·amino acid–AMP complex.**

*Key words:* *p*-Cl-phenylalanine; Phenylalanine; Phenylalanyl-tRNA synthetase; Pre-steady-state; tRNA; *Escherichia coli*

## 1. Introduction

The aminoacyl-tRNA synthetases catalyze the attachment of amino acids to their cognate tRNAs (for reviews see [1,2]). The phenylalanyl-tRNA synthetase (PheRS) of *Escherichia coli* is a heterotetrameric enzyme ($\alpha_2\beta_2$) which contains central antiparallel $\beta$-sheets flanked by $\alpha$-helices [3], a structural feature characteristic of class II tRNA synthetases [4,5]. It also contains all three amino acid sequence motifs diagnostic for class II synthetases [6]. PheRS catalyzes the attachment of phenylalanine to $tRNA^{Phe}$ in a two-step reaction: activation of the amino acid (Eqn. 1) followed by its attachment to tRNA (Eqn. 2):

$$E + Phe + ATP \overset{Mg^{2+}}{\rightleftharpoons} [E \cdot Phe\text{-}AMP] + PP_i \quad (1)$$

$$[E \cdot Phe\text{-}AMP] + tRNA^{Phe} \rightleftharpoons Phe\text{-}tRNA^{Phe} + AMP + E \quad (2)$$

Active site-engineered forms of PheRS with modified substrate specificity have previously been constructed [7] through replacement of Ala[294] in the $\alpha$ subunit (the crystal structure of PheRS from *Thermus thermophilus* suggests that the analogous residue in that enzyme, Ala*314*, is positioned at the bottom of a phenylalanine binding pocket; M. Safro, personal communication). These modifications lead to changes in the kinetics of both amino acid activation (Eqn. 1) and the overall aminoacylation reaction [8]. Comparison of the steady-state kinetic data for amino acid activation and aminoacylation suggested that reducing the catalytic efficiency of the former might increase the rate of tRNA charging [8]. However, steady-state kinetics can only provide indirect evidence for this conclusion, as they cannot completely separate the tRNA charging step (Eqn. 2) from the amino acid activation step (Eqn. 1). A more detailed understanding of the tRNA charging reaction can, however, be obtained by the use of pre-steady-state kinetics [9]. This approach has previously been employed to demonstrate how tyrosyl-tRNA synthetase from *Bacillus stearothermophilus* compromises between the rates of activation and tRNA charging in order to optimise the overall reaction rate [10].

The tRNA charging reaction of *E. coli* PheRS can be studied by stopped-flow fluorimetry [11,12]. In this work we present both steady-state and pre-steady-state kinetic data for the charging of $tRNA^{Phe}$ by wild-type and mutant PheRS-aminoacyl adenylates. The mutants chosen were those previously shown to possess altered kinetics of amino acid activation [8] and an additional mutant with an increased $K_m$ for phenylalanine, G191D, which is located in motif 2 [13]. Amino acid sequence alignments with class II tRNA synthetases whose structures have been solved at high resolution in the presence of tRNA or aminoacyl adenylates, the aspartyl- [5,14] and seryl- [15,16] tRNA synthetases, and comparison with the structure of *T. thermophilus* PheRS (M. Safro, personal communication), suggest that Gly[191] lies close to regions involved in tRNA, but not amino acid, binding [17]. Thus this mutant provides an interesting contrast to the mutations of Ala[294] which predominantly effect amino acid binding [7,8].

## 2. Materials and methods

### 2.1. Bacterial strains

The *E. coli* strains KA4/pKSC-Ala[294] and KA3/pKSC-Gly[294] were used for the homologous over-production of wild-type and A294G PheRS respectively [8]. Strains RR28 [7] and G1 [13] were used directly as the source of A294S PheRS and G191D PheRS, respectively.

### 2.2. Materials

L-[U-$^{14}$C]Phenylalanine was from Amersham International (Amersham, UK) and *p*-chloro-D,L-[1-$^{14}$C]phenylalanine from NEN-DuPont (Boston, USA). Phenylalanine, *p*-chloro-D,L-phenylalanine and *E. coli* $tRNA^{Phe}$ were from Sigma (St. Louis, USA).

### 2.3. Purification of PheRS

Cells were prepared for PheRS purification as described previously [8]. All PheRS proteins were then purified as previously described [8] except for the following modifications. Following gel filtration and concentration the samples were adjusted to 1 M $(NH_4)_2SO_4$ and applied to a Fractogel TSK 650 Butyl hydrophobic interaction column (Merck, Darmstadt, Germany). The column was developed with a 1 to 0 M $(NH_4)_2SO_4$ gradient, and the PheRS-containing fractions were pooled and further purified by anion exchange chromatography as before.

*Corresponding author. Fax. (41) (1) 632-1148.


*SSDI* 0014-5793(94)01454-X

*2.4. Preparation of PheRS aminoacyl adenylates*

The enzyme adenylate complex was prepared as follows. PheRS (2 μM) was incubated in a standard buffer (125 mM Tris-HCl, pH 7.7, 10 mM $MgCl_2$, 10 mM 2-mercaptoethanol, 0.1 mM dithiothreitol) with 5 mM ATP (pH 7.0), 170 μM [$^{14}$C]phenylalanine (20 μCi/μmol) or 850 μM [$^{14}$C]*p*-Cl-phenylalanine (8.7 μCi/μmol), and 2 units of inorganic pyrophosphatase at 25°C for 30 min, and the complex was then isolated as previously described [9].

*2.5. Preparation of aminoacyl-tRNA$^{Phe}$*

tRNA$^{Phe}$ charged with phenylalanine or *p*-Cl-phenylalanine was prepared as follows. A294G PheRS (10 nM) was incubated in standard buffer with 10 mM ATP (pH 7.0), 1 mM [$^{14}$C]*p*-Cl-phenylalanine (8.7 μCi/μmol) or 170 μM [$^{14}$C]phenylalanine (20 μCi/μmol), and 10 μM tRNA$^{Phe}$ for 10 min at 25°C. The product was then separated from enzyme and excess substrate by gel filtration on a Sephadex G-25 column (Pharmacia, Uppsala, Sweden) in 10 mM Bis-Tris (pH 6.0), 10 mM $MgCl_2$ and 10 mM 2-mercaptoethanol.

*2.6. Steady-state kinetic analyses*

All steady-state methods were as previously described [8] except that tRNA charging was performed using the procedure described by Avis et al. [9] with tyrosine replaced by either phenylalanine or *p*-Cl-phenylalanine.

*2.7. Direct observation of the reaction of tRNA$^{Phe}$ with PheRS-aminoacyl adenylates*

The reaction of wild-type *E. coli* PheRS-aminoacyl adenylate with tRNA$^{Phe}$ gives rise to two changes in intrinsic protein fluorescence. These have previously been attributed to the formation of a complex with tRNA$^{Phe}$ and the subsequent phenylalanylation of tRNA$^{Phe}$ [12]. The rates of these changes were monitored in an Applied Photophysics Model SX 17MV stopped-flow spectrophotometer (Applied Photophysics, Letherhead, UK). All experiments were performed at 25 ± 0.1°C. Excitation was at 285 nm, and emission at wavelengths above 320 nm was measured using a cut-off filter in the emission light path. One syringe contained 0.6 μM purified aminoacyl adenylate complex (see above), and the other 0.6–6 μM tRNA$^{Phe}$ in 250 mM Tris-HCl (pH 7.7). 60 μl volumes from each syringe were mixed and the reaction followed using the split time-base facility in order to allow the observation of both tRNA binding and amino acid transfer. All reactions were repeated at least 4 times and the data collected used to produce average traces. These were subsequently fitted to exponential equations using the Kaleidagraph data analysis program (Abelbeck Software).

*2.8. Measurement of the rate of product release using a stopped-flow apparatus*

The reaction of aminoacyl-tRNA$^{Phe}$ with PheRS was monitored in a stopped-flow spectrophotometer as described in the previous section. One syringe contained 0.25 μM PheRS in 10 mM Bis-Tris (pH 6.0) and the other 5 μM aminoacyl tRNA$^{Phe}$.

## 3. Results

*3.1. Steady-state tRNA charging kinetics*

The steady-state kinetic parameters with respect to tRNA$^{Phe}$ charging were determined for wild-type and mutant PheRS (Table 1). *p*-Cl-phenylalanine was only used as the amino acid substrate with A294G PheRS as this is the only of the mutants able to activate it [8]. Where phenylalanine was the amino acid substrate, the $K_m$ values were essentially the same in all cases, while the observed differences in $k_{cat}$ values follow the pattern previously observed for the aminoacylation reaction [8]. Where *p*-Cl-phenylalanine was used as the amino acid substrate the standard errors were high, possibly as a result of the lower efficiency of activation compared with phenylalanine (for A294G PheRS the values of $k_{cat}/K_m$ for pyrophosphate exchange are 0.55 $s^{-1}\cdot\mu M^{-1}$ for phenylalanine and 0.11 $s^{-1}\cdot\mu M^{-1}$ for *p*-Cl-phenylalanine).

Table 1
Steady-state tRNA charging kinetics of PheRS with tRNA$^{Phe}$[a]

| PheRS | Amino acid substrate | $K_m$ (μM) | $k_{cat}$($s^{-1}$) | $k_{cat}/K_m$ ($s^{-1}\cdot\mu M^{-1}$) |
|---|---|---|---|---|
| Wild-type | Phe | 0.35 ± 0.03 | 5.4 ± 0.52 | 15.5 ± 2.0 |
| A294G | Phe | 0.37 ± 0.01 | 4.2 ± 0.15 | 11.4 ± 0.4 |
| A294S | Phe | 0.34 ± 0.02 | 5.4 ± 0.43 | 15.9 ± 1.6 |
| A294G | *p*-Cl-Phe | 0.31 ± 0.13 | 2.8 ± 0.96 | 9.0 ± 4.9 |

[a]Performed at 37°C in order to allow comparison with previously determined steady-state parameters [8]. tRNA$^{Phe}$ concentrations were varied in the range 0.05–2 μM. Rate constants are quoted per mole of heterotetrameric enzyme as determined by active site titration. Results shown are means and standard errors of at least 3 experiments.

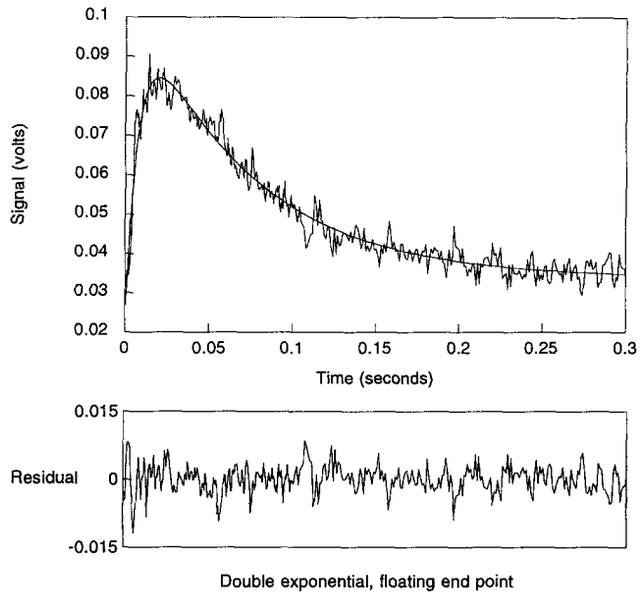


Fig. 1. Typical fluorescence trace observed on mixing equal volumes of PheRS-aminoacyl adenylate (0.3 μM) and tRNA$^{Phe}$ (0.3–3 μM) in a stopped-flow apparatus (25°C, 125 mM Tris-HCl, pH 7.7). The trace is recorded as a signal voltage, an increase in which is equivalent to a decrease in fluorescence (*F*). The trace is fitted to an exponential equation as described in the text. The accuracy of the fit is indicated by the residual ($F_{obs}-F_{calc}$).

*3.2. Reaction of isolated aminoacyl adenylate complexes with tRNA$^{Phe}$*

From previous experiments with wild-type PheRS it can be expected that the mixing of an aminoacyl adenylate complex with tRNA$^{Phe}$ will give rise to two fluorescence changes: the first as a result of tRNA binding and the second as result of product release [12]. Since product release itself is not rate-determining, the rate of the second fluorescence change will be determined by the rate of phenylalanine transfer [11]. A typical fluorescence trace observed upon mixing a preformed, isolated PheRS-aminoacyl adenylate with tRNA$^{Phe}$ is shown in Fig. 1. As expected, two fluorescence changes were observed: the first, a rapid exponential decrease (recorded as an increase in signal voltage) can be attributed to tRNA binding and occurs at a rate $k_{1obs}$. The second change can be attributed to product release and occurs at a rate, $k_{2obs}$, determined by the rate of phenylalanine transfer. Comparable changes were observed when the analogous experiment was performed with tyrosyl-tRNA synthetase from *B. stearothermophilus* [9]. Based on these observa-

Table 2
Pre-steady-state kinetic constants for reaction of $tRNA^{Phe}$ with wild-type and mutant enzyme-phenylalanyl adenylate complexes[a]

| PheRS | Amino acid substrate | $k_4$ ($s^{-1}$) | $k_{on}$ ($s^{-1} \cdot \mu M^{-1}$) | $k_{off}$ ($s^{-1}$) | $K_{tRNA}$[b] ($\mu M$) |
|---|---|---|---|---|---|
| Wild-type | Phe | 16.2 ± 1.5 | 37.1 ± 5.5 | 42.8 ± 7.4 | 1.2 ± 0.27 |
| A294G | Phe | 16.3 ± 1.3 | 42.1 ± 4.5 | 39.2 ± 7 | 0.93 ± 0.19 |
| A294G | *p*-Cl-Phe | 25.3 ± 1.3 | 42.6 ± 3.5 | 55.1 ± 5.2 | 1.3 ± 0.16 |
| A294S | Phe | 22.7 ± 2.4 | 68.9 ± 4.8 | 30.0 ± 8.1 | 0.44 ± 0.12 |
| G191D | Phe | 12.8 ± 1.1 | 22.8 ± 4.0 | 35.7 ± 4.1 | 1.6 ± 0.34 |

[a]Stopped-flow experiments performed at 25°C in standard 125 mM Tris-HCl buffer (pH 7.7) with 0.25 $\mu$M adenylate complex and 0.25–4 $\mu$M $tRNA^{Phe}$ (final concentrations). Rate and dissociation constants were calculated as described in the text. Results shown are means and standard errors of at least 3 experiments.
[b]$K_{tRNA} = k_{off}/k_{on}$.

tions and on earlier work with *E. coli* PheRS we can assume the same reaction scheme for the charging of $tRNA^{Phe}$ as for $tRNA^{Tyr}$ [9]:

$$E \cdot Phe\text{-}AMP + tRNA^{Phe} \underset{k_{off}}{\overset{k_{on}}{\rightleftharpoons}} E \cdot Phe\text{-}AMP \cdot tRNA^{Phe} \underset{k_{-4}}{\overset{k_4}{\rightleftharpoons}}$$

$$E \cdot Phe\text{-}tRNA^{Phe} \cdot AMP \xrightarrow{k_5} Phe\text{-}tRNA^{Phe} + AMP + E$$

Using this scheme, it is possible to calculate values for $k_4$, $k_{on}$, $k_{off}$, and $K_{tRNA}$ ($= k_{off}/k_{on}$) from $k_{1obs}$ and $k_{2obs}$ data [9]. This procedure was used to determine these kinetic parameters for wild-type and mutant PheRS with phenylalanine as amino acid substrate and also using *p*-Cl-phenylalanine with the A294G PheRS (Table 2). There is little variation in the dissociation constant $K_{tRNA}$ for the various complexes tested with the exception of the A294S PheRS-phenylalanyl adenylate. This suggests that the presence of an additional hydroxyl group in this mutant somehow results in a more favourable interaction with tRNA than is present in the wild-type. More variation is observed in the values of $k_4$, the rate constant for amino acid transfer. Both the *p*-Cl-Phe-A294G PheRS and the Phe-A294S PheRS mutant complexes have significantly faster rates of amino acid transfer, as shown by higher $k_4$ values, than the wild-type. Only a small increase in $K_{tRNA}$ and decrease in $k_4$ were observed for the Gly→$Asp^{191}$ mutant suggesting that this residue is not directly involved in the catalysis of tRNA charging.

### 3.3. Measurement of product release

While it has previously been shown that the release of Phe-$tRNA^{Phe}$ is not the rate-determining step for tRNA charging by wild-type PheRS [11,12], no such data exists for *p*-Cl-Phe-$tRNA^{Phe}$. To investigate this the reaction of A294G PheRS (0.25 $\mu$M) with an excess of isolated, preformed, *p*-Cl-Phe-$tRNA^{Phe}$ (5 $\mu$M) was monitored by stopped-flow fluorimetry. An exponential fluorescence change was observed with $k_{obs} = 60.9 \pm 2.1\ s^{-1}$, over two times the value of $k_4$ for the corresponding charging reaction, indicating that product release is not rate-determining.

Table 3
Gibbs' free energies of enzyme-bound species in the tRNA charging reaction, calculated relative to the enzyme-aminoacyl adenylate complex (E·Phe-AMP)

| PheRS | Amino acid substrate | $G_{E \cdot Phe\text{-}AMP \cdot tRNA}$ ($kcal \cdot mol^{-1}$) | $G_{[E \cdot Phe\text{-}tRNA \cdot AMP]\ddagger}$ ($kcal \cdot mol^{-1}$) |
|---|---|---|---|
| Wild-type | Phe | −8.07 | 7.72 |
| A294G | Phe | −8.22 | 7.57 |
| A294G | *p*-Cl-Phe | −8.03 | 7.50 |
| A294S | Phe | −8.67 | 6.93 |
| G191D | Phe | −7.90 | 8.03 |

### 3.4. Calculation of the energy levels of enzyme-bound species in the tRNA charging reaction

By substituting pre-steady-state dissociation and rate constants into thermodynamic equations it is possible to calculate the energy levels of the complex with tRNA and the transition state of amino acid transfer relative to the aminoacyl adenylate complex using the following equations [10]:

For the complex with tRNA,
$G_{E \cdot Phe\text{-}AMP \cdot tRNA} = RT \ln K_{tRNA}$,

and for the transition state of amino acid transfer,
$G_{[E \cdot Phe\text{-}tRNA \cdot AMP]\ddagger} = RT \ln(k_B T/h) - RT \ln(k_4/K_{tRNA})$

where $R$ is the gas constant, $T$ is the absolute temperature, $k_B$ is Boltzmann's constant, $h$ is Planck's constant and ‡ indicates the transition state. The calculated energies are shown in Table 3. The standard state is 1 M for all substrates. The free energy of activation of the transition state for wild-type PheRS (15.8 $kcal \cdot mol^{-1}$) is comparable to that for TyrRS (15.5 $kcal \cdot mol^{-1}$ [9]).

## 4. Discussion

The steady-state kinetic data for tRNA charging by PheRS provides no further information concerning the second step of the aminoacylation reaction than was known from previous studies. For the A294G mutant with *p*-Cl-phenylalanine as substrate, the steady state data suggests that this combination performs less well than the wild-type combination in contrast to the pre-steady-state data which clearly shows that it is, in fact, more efficient. This emphasises the problem associated with steady-state analysis of tRNA charging, that it cannot be entirely separated from the amino acid activation step. While this is less of a problem for mutants unaffected in amino acid activation [18] or when the tRNA itself is mutated [19], it may lead to misleading results where the rate of activation is changed as in the example described above. One commonly used means of circumventing this problem is to investigate the reaction of the free enzyme with tRNA [20,21]. With the exception of those aminoacyl-tRNA synthetases that bind tRNA

Table 4
Gibbs' free energies of enzyme-bound complexes in the aminoacylation reaction relative to the wild-type

| PheRS | Amino acid substrate | $\Delta\Delta G_{[E \cdot Phe\text{-}tRNA \cdot AMP]^{\ddagger}}$ (kcal·mol$^{-1}$)[a] | $\Delta\Delta G_{b(AA)}$ (kcal·mol$^{-1}$)[b] |
|---|---|---|---|
| A294G | Phe | 0 | +1.13[c] |
| A294G | *p*-Cl-Phe | −0.26 | +2.12[c] |
| A294S | Phe | −0.19 | +1.58[c] |
| G191D | Phe | +0.14 | +1.60[d] |

[a] Difference in the size of the energy barrier to transition state formation compared with the wild-type, $\Delta G_{[E \cdot Phe\text{-}tRNA \cdot AMP]^{\ddagger}} - \Delta G_{E \cdot Phe\text{-}AMP \cdot tRNA}$.
[b] Apparent difference in the energy of amino acid binding during steady- state pyrophosphate exchange, $\Delta\Delta G_{b(AA)} = -RT \ln\{(k_{cat}/K_m)_{mutant}/(k_{cat}/K_m)_{wild\text{-}type}\}$.
[c] $k_{cat}$ and $K_m$ values from Ibba et al. [8].
[d] This work.

prior to amino acid activation, such techniques can only provide indirect information on tRNA binding and no data on the rate of transfer. Since in most cases tRNA in fact binds to the enzyme–aminoacyl adenylate complex rather than the free enzyme such techniques may significantly overestimate $K_{tRNA}$, as was previously found with TyrRS [9]. Additionally, data concerning the effects of different amino acid substrates on tRNA charging are inaccessible using such methods.

The free energy values for the intermediates in the tRNA charging reaction can be used to compare the contribution of different enzyme side chains and substrates to the reaction. Table 4 shows the differences in free energy between wild-type and mutant reaction complexes for the formation of the transition state of amino acid transfer and the apparent differences in free energy for amino acid binding during activation calculated from steady-state pyrophosphate exchange data [22]. The lower activation barrier for the transition states of the *p*-Cl-Phe-A294G and Phe-A294S complexes correlates with apparently weaker binding of the amino acid to the enzyme as shown by the $\Delta\Delta G_{b(AA)}$ values. This is supported by the data for the mutation of Gly[191], which is not involved in amino acid binding, where no correlation between binding energy for the two steps is observed. Thus a compromise exists between amino acid activation and tRNA charging, because slowing down the first step increases the rate of the second step, possibly as a result of decreased stability of the PheRS·AA–AMP complex. Such a compromise has previously been demonstrated for Thr[51] mutants of *B. stearothermophilus* TyrRS where the rate constant for amino acid transfer decreases with increased stability of the TyrRS·Tyr–AMP complex [10]. No difference was observed in the energy of transition state formation between the wild-type and Phe-A294G complexes despite the apparent difference in amino acid binding. This may be explained by the difference in amino acid binding being insufficient to result in a detectable change in the free energy of transition state formation or may simply reflect the inadequecies of a steady-state analysis of amino acid activation. In order to resolve this question and to obtain data concerning the relative stability of the various PheRS·AA–AMP complexes it would now be necessary to undertake a detailed pre-steady-state analysis of amino acid activation by PheRS.

*Acknowledgements:* We would like to thank Gideon Schreiber for help with stopped-flow experiments, Mark Safro for sharing unpublished data with us concerning the structure of *T. thermophilus* PheRS, and Hannes Loferer for critical reading of the manuscript. M.I. was the recipient of a European Molecular Biology Organization Short-Term Fellowship.

## References

C[1] Carter Jr., C.W. (1993) Annu. Rev. Biochem. 62, 715–748.
[2] Delarue, M. and Moras, D. (1993) BioEssays 15, 675–687.
[3] Mosyak, L. and Safro, M. (1993) Biochimie 75, 1091–1098.
[4] Cusack, S., Berthet-Colominas, C., Härtlein, M., Nassar, N. and Leberman, R. (1990) Nature 347, 249–255.
[5] Ruff, M., Krishnaswamy, S., Boeglin, M., Poterszman, A., Mitschler, A., Podjarny, A., Rees, B., Thierry, J.-C. and Moras D. (1991) Science 252, 1682–1689.
[6] Eriani, G., Delarue, M., Poch, O., Gangloff, J. and Moras, D. (1990) Nature 347, 203–206.
[7] Kast, P. and Hennecke, H. (1991) J. Mol. Biol. 222, 99–124.
[8] Ibba, M., Kast, P. and Hennecke, H. (1994) Biochemistry 33, 7107–7112.
[9] Avis, J.M., Day, A.G., Garcia, G.A. and Fersht, A.R. (1993) Biochemistry 32, 5312–5320.
[10] Avis, J.M. and Fersht, A.R. (1993) Biochemistry 32, 5321–5326.
[11] Baltzinger, M. and Holler, E. (1982) Biochemistry 21, 2460–2467.
[12] Baltzinger, M. and Holler, E. (1982) Biochemistry 21, 2467–2476.
[13] Kast, P., Wehrli, C. and Hennecke, H. (1991) FEBS Lett. 293, 160–163.
[14] Cavarelli, J., Eriani, G., Rees, R., Ruff, M., Boeglin, M., Mitschler, A., Martin, F., Gangloff, J., Thierry, J.-C. and Moras, D. (1994) EMBO J. 13, 327–337.
[15] Belrhali, H., Yaremchuk, A., Tukalo, M., Larsen, K., Berthet-Colominas, C., Leberman, R., Beijer, B., Sproat, B., Als-Nielsen, J., Grübel, G., Legrand, J.-F., Lehmann, M., Cusack, S. (1994) Science 263, 1432–1436.
[16] Biou, V., Yaremchuk, A., Tukalo, M. and Cusack, S. (1994) Science 263, 1404–1410.
[17] Davis, M.W., Buechter, D.D. and Schimmel, P. (1994) Biochemistry 33, 9904–9911.
[18] Borel, F., Vincent, C., Leberman, R. and Härtlein, M. (1994) Nucleic Acids Res. 22, 2963–2969
[19] Sampson, J.R. and Saks, M.E. (1993) Nucleic Acids Res. 21, 4467–4475.
[20] Yarus, M. and Berg, P. (1969) J. Mol. Biol. 42, 171–189.
[21] Abrahams, J.P., Kraal, B. and Bosch, L. (1988) Nucleic Acids Res. 16, 10099–10108.
[22] Fersht, A.R. (1985) Enzyme Structure and Mechanism, W.H. Freeman and Co., New York.